


Science

AAAS

Robust, Tunable Biological Oscillations from Interlinked Positive and Negative Feedback LoopsTony Yu-Chen Tsai, *et al.**Science* **321**, 126 (2008);

DOI: 10.1126/science.1156951

The following resources related to this article are available online at www.sciencemag.org (this information is current as of July 10, 2008):

Updated information and services, including high-resolution figures, can be found in the online version of this article at:

<http://www.sciencemag.org/cgi/content/full/321/5885/126>

Supporting Online Material can be found at:

<http://www.sciencemag.org/cgi/content/full/321/5885/126/DC1>

This article **cites 44 articles**, 17 of which can be accessed for free:

<http://www.sciencemag.org/cgi/content/full/321/5885/126#otherarticles>

This article appears in the following **subject collections**:

Cell Biology

http://www.sciencemag.org/cgi/collection/cell_biol

Information about obtaining **reprints** of this article or about obtaining **permission to reproduce this article** in whole or in part can be found at:

<http://www.sciencemag.org/about/permissions.dtl>

Downloaded from www.sciencemag.org on July 10, 2008

10. Materials and methods are available as supporting material on Science Online.
11. U.N. Population Division (UNPD), *World Urbanization Prospects: The 2007 Revision Population Database* (UNPD, New York, 2007); available at <http://esa.un.org/unup> (accessed September 2007).
12. R. P. Cincotta, J. Wisniewski, R. Engelman, *Nature* **404**, 990 (2000).
13. D. M. Olson *et al.*, *Bioscience* **51**, 933 (2001).
14. A. de Sherbinin, *Oryx* **42**, 26 (2008).
15. UNEP-WCMC, *Prototype Nationally Designated Protected Areas Database* (WCMC/UNEP, Cambridge, 2003); available at www.unep-wcmc.org/protected_areas/data/nat.htm (accessed September 2007).
16. A. N. James, M. J. B. Green, J. R. Paine, *Global Review of Protected Area Budgets and Staff* (WCMC, Cambridge, 1999).
17. A. Balmford, K. J. Gaston, S. Blyth, A. James, V. Kapos, *Proc. Natl. Acad. Sci. U.S.A.* **100**, 1046 (2003).
18. A. James, K. J. Gaston, A. Balmford, *Bioscience* **51**, 43 (2001).
19. GEF, *GEF Biodiversity Strategy in Action* (GEF, Washington, DC, 2006).
20. GEF, *The GEF Project Database* (GEF, Washington, DC, 2008); available at <http://gefonline.org/home.cfm> (accessed March 2008).
21. W. D. Newmark, J. L. Hough, *Bioscience* **50**, 585 (2000).
22. G. W. Luck, *Biol. Rev. Camb. Philos. Soc.* **82**, 607 (2007).
23. K. K. Karanth, L. M. Curran, J. D. Reuning-Scherer, *Biol. Conserv.* **128**, 147 (2006).
24. J. S. Brashares, P. Arcese, M. K. Sam, *Proc. R. Soc. London B. Biol. Sci.* **268**, 2473 (2001).
25. A. T. Hudak, D. H. K. Fairbanks, B. H. Brockett, *Agric. Ecosyst. Environ.* **101**, 307 (2004).
26. R. DeFries, A. Hansen, A. C. Newton, M. C. Hansen, *Ecol. Appl.* **15**, 19 (2005).
27. E. W. Sanderson *et al.*, *Bioscience* **52**, 891 (2002).
28. R. DeFries, A. Hansen, B. L. Turner, R. Reid, J. G. Liu, *Ecol. Appl.* **17**, 1031 (2007).
29. Overlapping buffers in multiple PAs were combined for analysis, which decreased the sample of 306 PAs to 284 buffer areas. Countries and ecoregions with one park were excluded from statistical analysis of median buffer growth rates, although results did not vary with their inclusion.
30. Supported by NSF OISE-0502340 and the J. S. McDonnell Foundation (G.W.), the Hellman Fund (J.S.B.) and the University of California at Berkeley. We thank A. Balmford, A. Bruner, P. Coppolillo, C. Golden, C. Kremen, R. Kuriyan, J. Scharlemann, A. R. E. Sinclair, C. Stoner, two anonymous reviewers, and the Geospatial Imaging and Informatics Facility (GIIF), Museum of Vertebrate Zoology (MVZ), and Department of Environmental Science, Policy, and Management (ESPM) at the University of California at Berkeley. The authors declare no competing financial interests.

Supporting Online Material

www.sciencemag.org/cgi/content/full/321/5885/123/DC1
Materials and Methods
SOM Text
Figs. S1 to S3
Table S1
References

9 April 2008; accepted 4 June 2008
10.1126/science.1158900

Robust, Tunable Biological Oscillations from Interlinked Positive and Negative Feedback Loops

Tony Yu-Chen Tsai,^{1*} Yoon Sup Choi,^{1,2*} Wenzhe Ma,^{3,4} Joseph R. Pomeroy,⁵ Chao Tang,^{3,4} James E. Ferrell Jr.^{1†}

A simple negative feedback loop of interacting genes or proteins has the potential to generate sustained oscillations. However, many biological oscillators also have a positive feedback loop, raising the question of what advantages the extra loop imparts. Through computational studies, we show that it is generally difficult to adjust a negative feedback oscillator's frequency without compromising its amplitude, whereas with positive-plus-negative feedback, one can achieve a widely tunable frequency and near-constant amplitude. This tunability makes the latter design suitable for biological rhythms like heartbeats and cell cycles that need to provide a constant output over a range of frequencies. Positive-plus-negative oscillators also appear to be more robust and easier to evolve, rationalizing why they are found in contexts where an adjustable frequency is unimportant.

The mammalian heart rate is normally established by the sino-atrial node. The node generates constant-amplitude action potentials at a tunable frequency of ~50 to 150 action potentials per minute, depending on the body's oxygen demands. The cell cycle oscillator may also require this combination of an adjustable frequency and invariant amplitude. The period of the cell cycle ranges from about 10 min in rapidly dividing embryos to tens of hours in rapidly dividing somatic cells (and longer in slowly dividing somatic cells), but variations in the amplitude

[the peak concentration of active cyclin-dependent kinase-1 (CDK1)] of the oscillations seem neither necessary nor desirable.

Two basic types of circuits have been proposed for biological oscillators: (i) those that contain both positive and negative feedback loops and (ii) those containing only negative feedback (Table 1) (1–6). Both the sino-atrial node oscillator and the cell cycle oscillator fall into the positive-plus-negative feedback class, suggesting that this design might be better suited for generating oscillations with a tunable frequency and constant amplitude.

We tested this idea through computational studies, beginning with an ordinary differential equation model of CDK1 oscillations in the *Xenopus* embryonic cell cycle (7). The model includes a negative feedback loop [active CDK1 brings about its inactivation through the anaphase-promoting complex (APC)] and a pair of positive feedback loops (active CDK1 activates its activator Cdc25 and inactivates its inhibitor Wee1) (Fig. 1A). We specified the strength of the posi-

tive feedback through a parameter r , the ratio of the activities of Cdc25 and Wee1 in interphase versus M phase. Because the rate of cyclin synthesis determines the frequency of CDK1 oscillations in *Xenopus* embryos (7, 8), we varied the cyclin synthesis rate constant k_{synth} in the model and determined how the amplitude and frequency of the oscillations were affected by this variation.

In the negative feedback-only version of the model ($r = 1$ in Fig. 1, B and C), a relatively small range of k_{synth} values yielded oscillations. Plotting the amplitude and frequency of the oscillations on a log-log plot yielded a tight, inverted U-shaped curve (Fig. 1B). The range of frequencies over which the oscillator functioned was small (1.7-fold), and even within this range, the frequency could not be adjusted without compromising the amplitude substantially.

Adding positive feedback markedly changed the amplitude/frequency relation (Fig. 1, B and C). At a biologically realistic feedback strength of $r = 10$ (9–11), the oscillator functioned over a 4900-fold range of frequencies (Fig. 1B, green points). Over much of this range, the frequency of the oscillator was linearly proportional to k_{synth} , and the amplitude was approximately constant (Fig. 1, B and C). Thus, positive feedback provided a highly tunable frequency and robust amplitude.

Something other than the cyclin synthesis rate may tune the frequencies of some cell cycles. We therefore asked whether the negative feedback-only oscillator might operate over a wider range of frequencies if one of the model's other 20 parameters were varied. This was not the case; invariably, the oscillator operated over only a narrow frequency range. Of course if all of the rate constants were multiplied by the same factor (equivalent to scaling the units of time), the oscillator's frequency could be varied without changing the amplitude. However, this type of coordinated regulation is not relevant to any of the biological oscillators that we are familiar with (Table 1).

¹Department of Chemical and Systems Biology, Stanford University School of Medicine, Stanford, CA 94305–5174, USA.

²School of Interdisciplinary Bioscience and Bioengineering, Pohang University of Science and Technology, Pohang, 790-784, Republic of Korea. ³Center for Theoretical Biology, Peking University, Beijing, 100871, China. ⁴California Institute for Quantitative Biosciences, University of California, San Francisco, CA 94143–2540, USA. ⁵Department of Biology, Indiana University, Bloomington, IN 47405, USA.

*These authors contributed equally to this work.

†To whom correspondence should be addressed. E-mail: james.ferrell@stanford.edu

Both the tunable frequency and constant amplitude of the positive-plus-negative feedback cell cycle model arise because the system behaves like a relaxation oscillator (12–15). Relaxation oscillators are built on a hysteretic switch, and experimental studies have shown that in *Xenopus* extracts the response of the CDK1/Cdc25/Wee1/Myt1 positive feedback loop is hysteretic, resembling that shown in Fig. 2A (16, 17).

To see how relaxation oscillations can arise from a hysteretic switch and to see why this permits a tunable period and constant amplitude, assume that a cell cycle begins with no cyclin B and no active CDK1 and that cyclin B synthesis is slow relative to the phosphorylation and dephosphorylation reactions that allow the hysteretic switch to approach its steady state (Fig. 2A). As cyclin B accumulates, the system moves up the

lower branch of the stimulus/response curve, and the CDK1 activity slowly rises (Fig. 2, A and B, segments 0 and 1). Ultimately, the branch terminates and the system switches (“relaxes”) to the other branch (Fig. 2, A and B, segment 2).

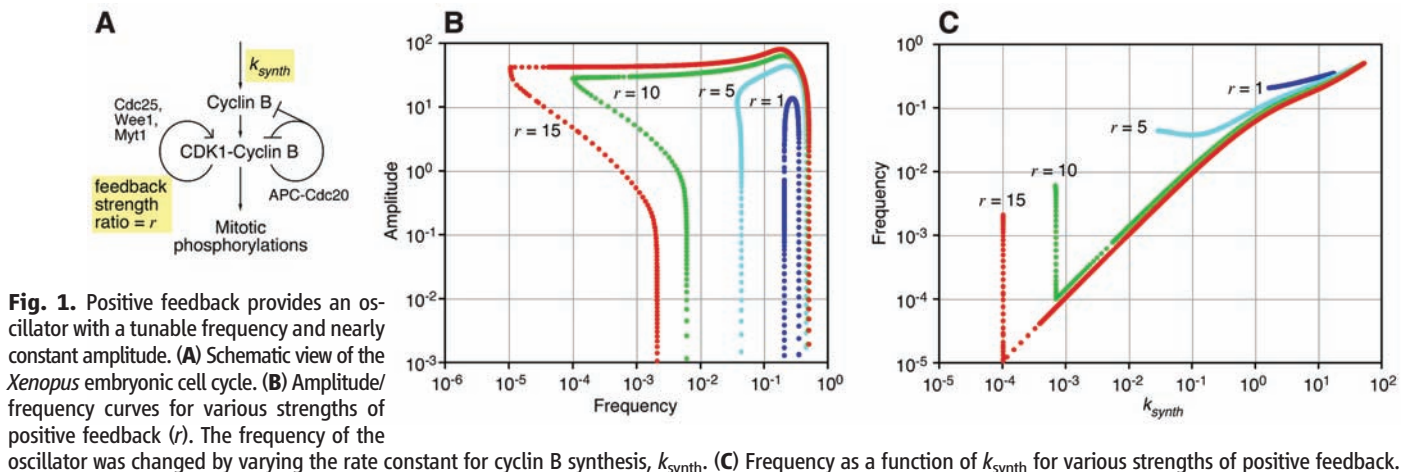
Now assume that at this higher, mitotic level of CDK1 activity, the APC is turned on and the cyclin B concentration begins to fall slowly. The system progresses down the upper branch of the stimulus/response curve (Fig. 2, A and B, segment 3) until the branch terminates and the system switches to the lower branch (Fig. 2, A and B, segment 4). The APC turns back off, cyclin B reaccumulates, and the cycle starts over. Thus, oscillations in this system essentially represent a walk around the hysteretic steady-state stimulus/response loop. The frequency of the oscillator is determined by how rapid the walk is, and the amplitude (the height of the loop) is constant.

In reality, the rate of cyclin B destruction by the APC is not slow compared with the phosphorylation and dephosphorylation reactions (7). This fact is incorporated into the cell cycle model examined here, and it makes the orbits of the oscillator overshoot the hysteretic loop (Fig. 2C). Nevertheless, the model still behaves much like a relaxation oscillator, especially at low k_{synth} values (Fig. 2, C and D).

To test the generality of the idea that positive feedback enables an oscillator to have a tunable frequency and constant amplitude, we examined several other oscillator models, including five negative feedback-only models: (i) the Goodwin oscillator, a well-studied model relevant to circadian oscillations (18, 19); (ii) the Repressilator, a transcriptional triple-negative feedback loop constructed in *Escherichia coli* (20); (iii) the “Pentilator,” a Repressilator with five (rather than three) repressors; (iv) the Metabolator (21), a synthetic metabolic oscillator; and (v) the Frzillator, a model of the control of gliding motions in myxobacteria (22). In four of the cases (Goodwin, Repressilator, Pentilator, and Metabolator), the amplitude/frequency curves were inverted U-shaped curves similar to that seen for the negative feedback-only cell cycle model (Figs. 1B and 3A). In the case of the

Table 1. Positive feedback loops in biological oscillators.

Oscillator	Period	Positive feedback	Refs.
Sino-atrial pacemaker	~1 s	Depolarization → Na ⁺ channel activation → depolarization	(29)
Calcium spikes	~100 s	Cytoplasmic Ca ²⁺ → PLC → IP ₃ → cytoplasmic Ca ²⁺ Cytoplasmic Ca ²⁺ → IP ₃ R → cytoplasmic Ca ²⁺ Cytoplasmic Ca ²⁺ → IP ₃ R -l ER Ca ²⁺ -l SOC → cytoplasmic Ca ²⁺	(25, 30, 31)
Myxobacterial gliding	~10 min	None known	(22)
Animal cell cycle (<i>Xenopus laevis</i> embryos)	~30 min	Cdk1 → Cdc25 → Cdk1 Cdk1 -l Wee1 -l Cdk1 Cdk1 -l Myt1 -l Cdk1	(32, 33)
Somitogenesis	~30 min	DeltaC → Notch → DeltaC	(34)
Yeast cell cycle (<i>S. cerevisiae</i>)	~2 hours	CLN1,2 transcription → CDK1 → CLN1,2 transcription CDK1 -l Sic1 -l CDK1 CDK1 -l Cdh1 -l CDK1	(6, 35–39)
NF-κB responses	~100 min	None known	(40, 41)
p53 responses	~100 min	p53 → PTEN -l Akt → Mdm2 -l p53 p53 → p21 -l Cdk2 -l Rb -l Mdm2 -l p53	(42, 43)
Animal cell cycle (somatic cells)	~24 hours	CDK2 -l Rb → E2F → CDK2 Cdk1 → Cdc25 → Cdk1 Cdk1 -l Wee1 -l Cdk1 Cdk1 -l Myt1 -l Cdk1	(44)
Circadian rhythm (mammals)	~24 hours	BMAL1 → Rora → BMAL1	(45)
Circadian rhythm (<i>Drosophila</i>)	~24 hours	CLK → PDP1 → CLK	(45)
Circadian rhythm (fungi)	~24 hours	FRQ → WC-1 → FRQ	(46)
Circadian rhythm (cyanobacteria)	~24 hours	KaiC-SP -l KaiA -l KaiC-SP	(26)



Frzillator, the legs of the curve were truncated; the oscillator had a nonzero minimal amplitude (Fig. 3A). For all five of the negative feedback-only models, the oscillators functioned over only a narrow range of frequencies (Fig. 3A).

We also examined four positive-plus-negative feedback oscillators: (i) the van der Pol oscillator, inspired by studies of vacuum tubes (12); (ii) the Fitzhugh-Nagumo model of propagating action potentials (23, 24); (iii) the Meyer-Stryer model of calcium oscillations (25); and (iv) a model of circadian oscillations in the cyanobacterial KaiA/B/C system (26–28). In each case, we obtained a flat, wide amplitude/frequency curve (Fig. 3B). Thus, a tunable frequency plus constant amplitude can be obtained from many different positive-plus-negative feedback models; this feature is not peculiar to one particular topology or parameterization.

These findings rationalize why the positive-plus-negative feedback design might have been selected through evolution in cases where a tunable frequency and constant amplitude are important, such as heartbeats and cell cycles. However, it is not clear that an adjustable frequency would be advantageous for circadian oscillations, because frequency is fixed at one cycle per day. Nevertheless, the cyanobacterial circadian oscillator appears to rely on positive feedback (26), and positive feedback loops have been postulated for other circadian oscillators as well (Table 1). This raises the question of whether the positive-plus-negative feedback design might offer additional advantages.

One possibility is that the positive-plus-negative feedback design permits oscillations over a wider range of enzyme concentrations and kinetic constant values, making the oscillator easier to evolve and more robust to variations in its imperfect components. We tested this idea through a Monte Carlo approach. We formulated three simple oscillator models: (i) a three-variable triple negative feedback loop with no additional feedback (Fig. 4A), (ii) one with added positive feedback (Fig. 4B), or (iii) one with added negative feedback (Fig. 4C). We generated random parameter sets for the models and then for each set determined whether the model produced limit cycle oscillations. We continued generating parameter sets until we had amassed 500 that gave oscillations.

For the negative feedback-only model, 500 out of 138,785 parameter sets (0.36%) yielded oscillations (Fig. 4D). For the positive-plus-negative feedback model, oscillatory parameter sets were found at a higher rate: 500 out of 23,848 parameter sets (2.1%) if we assumed weak positive feedback and 500 out of 9854 sets (5.1%) for strong positive feedback (Fig. 4D). The negative-plus-negative feedback model yielded oscillations at a lower rate than even the negative feedback-only model: 500 out of 264,672 parameter sets (0.19%) for the weaker feedback strength and 500 out of 583,263 (0.086%) for the stronger feedback. This is probably because the short negative feedback loop stabilizes the output of *A*, making it difficult for changes in *C*'s activity to be propa-

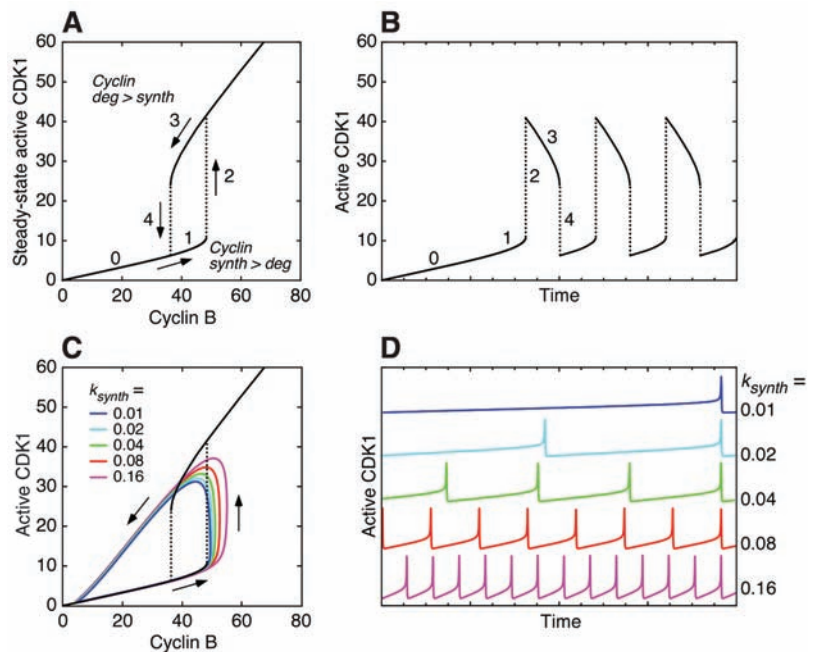


Fig. 2. From a hysteretic switch to a relaxation oscillator. (A) Hysteretic steady-state response of CDK1 to cyclin B, on the basis of previous experimental studies (16, 17). (B) CDK1 activation and inactivation in the limit of slow cyclin B synthesis and degradation. (C and D) Cell cycle model run with biologically realistic parameters, showing a looser relation between the oscillations and the hysteretic steady-state response.

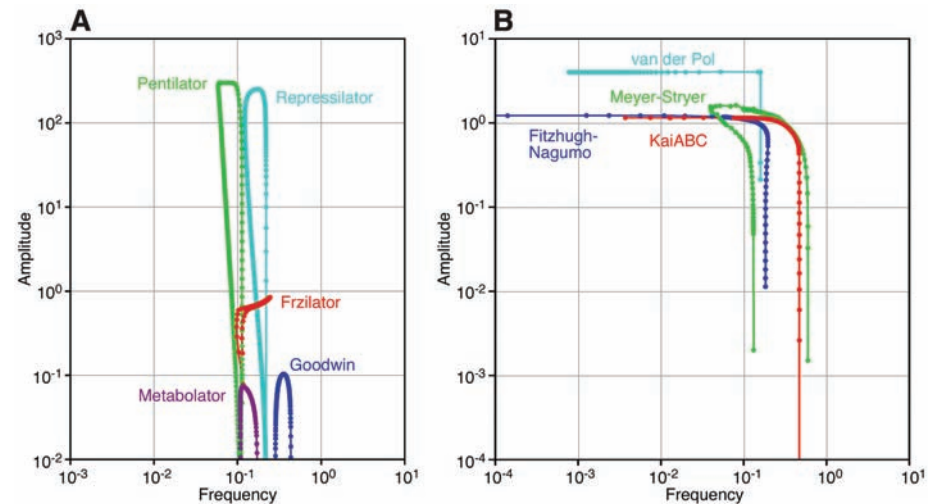


Fig. 3. Amplitude/frequency curves for various legacy oscillators. (A) Negative feedback-only models. (B) Positive-plus-negative feedback models.

gated onward. Thus, the positive-plus-negative feedback design was substantially more robust, by this measure, than either the negative feedback-only model or the negative-plus-negative feedback model.

The random parameter sets also provided a further test of the hypothesis that the positive-plus-negative design allows for a tunable frequency. For each oscillator set, we varied one parameter (k_3) and calculated amplitude/frequency curves and operational frequency ranges. For the negative feedback-only and the negative-plus-negative

feedback models, all of the oscillatory parameter sets yielded narrow, inverted U-shaped amplitude/frequency curves with small operational frequency ranges (Fig. 4, E and F, and fig. S1). In contrast, many of the amplitude/frequency curves for the positive-plus-negative feedback model were flat and wide, with large operational frequency ranges (Fig. 4, E and F). Thus, the positive-plus-negative design provided the possibility of a tunable frequency and near-constant amplitude.

The frequent presence of positive feedback loops in natural biological oscillators suggests

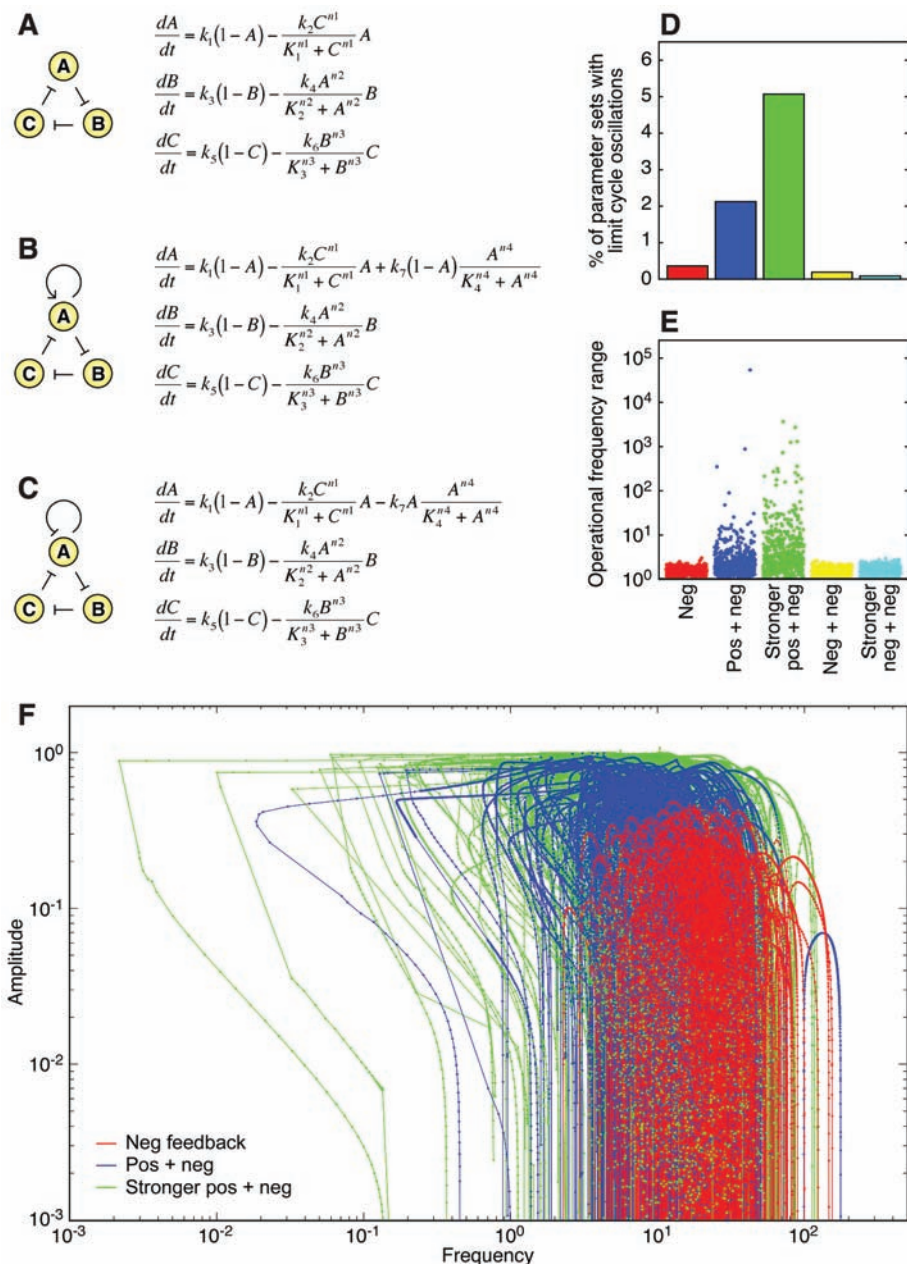


Fig. 4. Randomly parameterized oscillator models. **(A)** Negative feedback-only. *A*, *B*, and *C*, the fractions of proteins *A*, *B*, and *C* that are active; *K_i*, median effective concentration values of the Hill functions; *n_i*, Hill coefficients; *k_i*, rate constants. **(B)** Positive-plus-negative feedback. **(C)** Negative-plus-negative feedback. **(D)** Percentage of parameter sets that yielded limit cycle oscillations. For the positive-plus-negative and negative-plus-negative models, we looked at two ranges of feedback strengths: (i) *k₇* = 0 to 100 (weak) and (ii) *k₇* = 500 to 600 (strong). **(E)** Operational frequency ranges for the oscillators. Each point represents *freq_{max}*/*freq_{min}* for one of the 2500 parameter sets that produced oscillations, with *k₃* as the bifurcation parameter. Mean operational frequency ranges were 1.6, 370, 63, 1.6, and 1.6. Medians were 1.6, 2.2, 3.3, 1.6, and 1.6. **(F)** Amplitude/frequency curves for the randomly parameterized models. We show 300 out of 500 curves for the negative feedback-only model (red) and the positive-plus-negative feedback model with weak (blue) or strong (green) positive feedback. Curves for the negative-plus-negative feedback model are shown in fig. S1.

that this type of circuit possesses some performance advantages over simple negative feedback loops. The present work demonstrates two such advantages: (i) the ability to tune the oscillator's frequency without changing its amplitude and (ii) a greater robustness and reliability.

References and Notes

1. C. D. Thron, *Biophys. Chem.* **57**, 239 (1996).
2. A. Goldbeter *et al.*, *Chaos* **11**, 247 (2001).
3. J. J. Tyson, K. C. Chen, B. Novak, *Curr. Opin. Cell Biol.* **15**, 221 (2003).
4. P. Smolen, D. A. Baxter, J. H. Byrne, *Am. J. Physiol.* **274**, C531 (1998).

5. A. Goldbeter, *Nature* **420**, 238 (2002).
6. F. R. Cross, *Dev. Cell* **4**, 741 (2003).
7. J. R. Pomerening, S. Y. Kim, J. E. Ferrell Jr., *Cell* **122**, 565 (2005).
8. R. S. Hartley, R. E. Rempel, J. L. Maller, *Dev. Biol.* **173**, 408 (1996).
9. A. Kumagai, W. G. Dunphy, *Cell* **70**, 139 (1992).
10. P. R. Mueller, T. R. Coleman, W. G. Dunphy, *Mol. Biol. Cell* **6**, 119 (1995).
11. S. Y. Kim, E. J. Song, K. J. Lee, J. E. Ferrell Jr., *Mol. Cell Biol.* **25**, 10580 (2005).
12. B. van der Pol, J. van der Mark, *Philos. Mag.* **6** (suppl.), 763 (1928).
13. H. S. Hahn, A. Nitzan, P. Ortoleva, J. Ross, *Proc. Natl. Acad. Sci. U.S.A.* **71**, 4067 (1974).
14. C. R. Nave, *Hyperphysics* (1995), (<http://hyperphysics.phy-astr.gsu.edu/Hbase/electronic/relaxo.html>).
15. S. H. Strogatz, *Nonlinear Dynamics and Chaos: With Applications to Physics, Biology, Chemistry, and Engineering* (Westview, Cambridge MA, 1994).
16. W. Sha *et al.*, *Proc. Natl. Acad. Sci. U.S.A.* **100**, 975 (2003).
17. J. R. Pomerening, E. D. Sontag, J. E. Ferrell Jr., *Nat. Cell Biol.* **5**, 346 (2003).
18. B. C. Goodwin, Ed. *Oscillatory Behavior in Enzymatic Control Processes*, vol. 3 (Permagon, Oxford, 1965), pp. 425–438.
19. P. Ruoff, S. Mohsenzadeh, L. Rensing, *Naturwissenschaften* **83**, 514 (1996).
20. M. B. Elowitz, S. Leibler, *Nature* **403**, 335 (2000).
21. E. Fung *et al.*, *Nature* **435**, 118 (2005).
22. O. A. Igoshin, A. Goldbeter, D. Kaiser, G. Oster, *Proc. Natl. Acad. Sci. U.S.A.* **101**, 15760 (2004).
23. R. FitzHugh, *Biophys. J.* **1**, 445 (1961).
24. J. Nagumo, S. Arimoto, S. Yoshizawa, *Proc. IRE* **50**, 2061 (1964).
25. T. Meyer, L. Stryer, *Proc. Natl. Acad. Sci. U.S.A.* **85**, 5051 (1988).
26. M. J. Rust, J. S. Markson, W. S. Lane, D. S. Fisher, E. K. O'Shea, *Science* **318**, 809 (2007); published online 4 October 2007, 10.1126/science.1148596.
27. M. Nakajima *et al.*, *Science* **308**, 414 (2005).
28. T. Nishiwaki *et al.*, *EMBO J.* **26**, 4029 (2007).
29. A. L. Hodgkin, A. F. Huxley, *J. Physiol.* **117**, 500 (1952).
30. R. S. Lewis, *Annu. Rev. Immunol.* **19**, 497 (2001).
31. M. J. Berridge, *Novartis Found. Symp.* **239**, 52 (2001).
32. B. Novak, J. J. Tyson, *J. Cell Sci.* **106**, 1153 (1993).
33. J. J. Tyson, B. Novak, *J. Theor. Biol.* **210**, 249 (2001).
34. A. Mara, S. A. Holley, *Trends Cell Biol.* **17**, 593 (2007).
35. K. Levine, A. H. Tinkelenberg, F. Cross, *Prog. Cell Cycle Res.* **1**, 101 (1995).
36. J. M. Bean, E. D. Siggia, F. R. Cross, *Mol. Cell* **21**, 3 (2006).
37. D. Stuart, C. Wittenberg, *Genes Dev.* **9**, 2780 (1995).
38. L. Dirick, K. Nasmyth, *Nature* **351**, 754 (1991).
39. K. C. Chen *et al.*, *Mol. Biol. Cell* **15**, 3841 (2004).
40. A. Hoffmann, A. Levchenko, M. L. Scott, D. Baltimore, *Science* **298**, 1241 (2002).
41. D. E. Nelson *et al.*, *Science* **306**, 704 (2004).
42. R. Lev Bar-Or *et al.*, *Proc. Natl. Acad. Sci. U.S.A.* **97**, 11250 (2000).
43. G. Lahav *et al.*, *Nat. Genet.* **36**, 147 (2004).
44. L. A. Buttitta, B. A. Edgar, *Curr. Opin. Cell Biol.* **19**, 697 (2007).
45. M. Gallego, D. M. Virshup, *Nat. Rev. Mol. Cell Biol.* **8**, 139 (2007).
46. K. Lee, J. J. Loros, J. C. Dunlap, *Science* **289**, 107 (2000).
47. We thank E. Sontag, A. Millar, and B. Novak for helpful discussions; J. Hasty for communicating unpublished results; and J. Ubersax and G. Anderson for comments on the manuscript. This work was supported by grants from NIH (GM61726 and GM77544), by the Li Foundation, and by a Korea Science and Engineering Foundation grant from the Korean government (No. R15-2004-033-05002-0).

Supporting Online Material

www.sciencemag.org/cgi/content/full/321/5885/126/DC1
SOM Text
Fig. S1
Table S1
References

25 February 2008; accepted 9 June 2008
10.1126/science.1156951